Title

Spatially explicit feedbacks between seagrass meadow structure, sediment and light: Habitat suitability for seagrass growth

Authors

Carr, Joel A
D'Odorico, Paolo
McGlathery, Karen J
et al.

Publication Date

2016-07-01

DOI

10.1016/j.advwatres.2015.09.001

Peer reviewed

Advances in Water Resources 93 (2016) 315–325

Contents lists available at ScienceDirect

Advances in Water Resources

journal homepage: www.elsevier.com/locate/advwatres

Spatially explicit feedbacks between seagrass meadow structure, sediment and light: Habitat suitability for seagrass growth

Joel A. Carr[a,b,*], Paolo D'Odorico[a], Karen J. McGlathery[a], Patricia L. Wiberg[a]

[a] Department of Environmental Sciences, University of Virginia, 291 McCormick Rd, Clark Hall, Charlottesville, VA 22904, United States
[b] Patuxent Wildlife Research Center, U.S. Geological Survey, 12100 Beech Forest Road, Laurel, MD 20708, United States

ARTICLE INFO

Article history:
Available online 10 September 2015

Keywords:
Seagrass
Resilience
Shear partitioning
Bistable dynamics
Modeling
Sediment resuspension

ABSTRACT

In shallow coastal bays where nutrient loading and riverine inputs are low, turbidity, and the consequent light environment are controlled by resuspension of bed sediments due to wind-waves and tidal currents. High sediment resuspension and low light environments can limit benthic primary productivity; however, both currents and waves are affected by the presence of benthic plants such as seagrass. This feedback between the presence of benthic primary producers such as seagrass and the consequent light environment has been predicted to induce bistable dynamics locally. However, these vegetated areas influence a larger area than they footprint, including a barren adjacent downstream area which exhibits reduced shear stresses. Here we explore through modeling how the patchy structure of seagrass meadows on a landscape may affect sediment resuspension and the consequent light environment due to the presence of this sheltered region. Heterogeneous vegetation covers comprising a mosaic of randomly distributed patches were generated to investigate the effect of patch modified hydrodynamics. Actual cover of vegetation on the landscape was used to facilitate comparisons across landscape realizations. Hourly wave and current shear stresses on the landscape along with suspended sediment concentration and light attenuation characteristics were then calculated and spatially averaged to examine how actual cover and mean water depth affect the bulk sediment and light environment. The results indicate that an effective cover, which incorporates the sheltering area, has important controls on the distributions of shear stress, suspended sediment, light environment, and consequent seagrass habitat suitability. Interestingly, an optimal habitat occurs within a depth range where, if actual cover is reduced past some threshold, the bulk light environment would no longer favor seagrass growth.

Published by Elsevier Ltd.

1. Introduction

In shallow coastal bays that lack riverine discharge, sediment dynamics are dominated by internal resuspension due to wind-waves and tidal currents [1]. Primary production in coastal bays, typically dominated by benthic plants (seagrasses and algae) can be severely limited when sediment resuspension is high, resulting in low light environments [2]. This is more important for high light requirement species such as seagrass, which need roughly 20% of incident light at the seafloor for survival [2–6].

Both currents and waves are affected by the presence of benthic plants [7] and the magnitude and importance of resuspension may increase when rooted vegetation is absent due to the lack of the sediment stabilizing effects of the plants [8–10]. This reduction in sediment resuspension due to the presence of benthic primary producers results in a positive feedback between vegetation and sediment suspension/deposition and a more beneficial light environment for seagrass growth [7]. Positive feedbacks between the state of the system (e.g., seagrass cover) and limiting resources (e.g., light) can induce the emergence of alternate stable states in ecosystem dynamics [11]. In the case of seagrass ecosystems, these alternate states would be exhibited by either bare sediment beds with high suspended loads and poor light environments for seagrass growth, or seagrass meadows with relatively clear water and enough light penetration through the water column to sustain seagrass growth.

The emergence of alternate states in ecosystems is important as these systems tend to behave in nonlinear manners, with small changes in environmental conditions potentially causing rapid shifts between alternate states. Ecosystems with alternate state dynamics exhibit limited resilience [12,13]. Recovery from disturbances can only occur if the disturbance intensity (e.g., fraction of seagrass covered landscape disturbed) does not exceed some critical threshold. Beyond that threshold of disturbance intensity, the system would move into the attraction domain of the alternate stable state (a bare landscape). Moreover, once the external forcing causing the disturbance is eliminated, the system would then remain within the

* Corresponding author at: Patuxent Wildlife Research Center, U.S. Geological Survey, 12100 Beech Forest Road, Laurel, MD 20708, United States. Tel.: +1 3014975710.
E-mail address: jac6t@virginia.edu (J.A. Carr).

http://dx.doi.org/10.1016/j.advwatres.2015.09.001
0309-1708/Published by Elsevier Ltd.

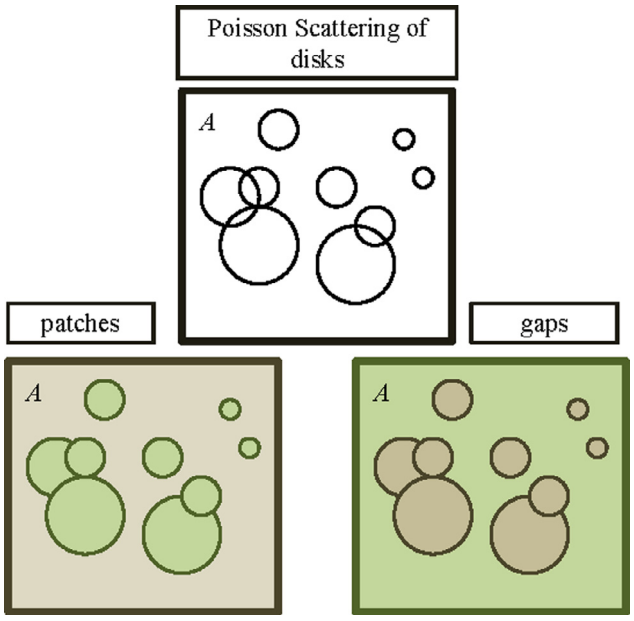

Fig. 1. Generation of landscape realizations from a spatial Poisson point process, scattering overlapping disks of radius r, sampled from an exponential distribution with mean of 1 m, on an area A, and then interpreting those disks as either patches on a bare seafloor or gaps in a continuous meadow landscape.

attractive domain of the alternate state and be unable to recover to its pre-disturbance state [14–16]. This alternate (bare) state possesses resilience as well, in that below some threshold level of disturbance (seeding, seagrass transplantation) the system will remain in the attractive domain of that state. As such, the emergence of bistable dynamics in seagrass ecosystems has significant implications for restoration, maintenance, and resilience of these ecosystems [17,18].

While a number of authors have investigated the dependence of hydrodynamic conditions on shoot density within homogenous seagrass meadows [17–23], only few studies [24–26] have addressed these interactions on a larger scale within a mosaic of seagrass patches and bare sediment. Some authors have linked disturbances and environmental conditions to meadow patchiness and general meadow landscape patterns [27–33], however, the consequential effect of meadow patch density on sediment resuspension and the resultant light environment as it pertains to seagrass persistence, growth and the emergence of alternate state dynamics has been neglected. Here, we use a simplified representation of seagrass modified hydrodynamics to explore how the patchy structure of seagrass meadows on a landscape may affect sediment resuspension, the consequent light environment, and the emergence of landscape scale alternate state dynamics under tidal and wind-wave forcing.

2. Methods

2.1. Modeling approach

We generated heterogeneous vegetation covers comprising a mosaic of circular patches randomly distributed according to a two-dimensional Poisson process, with rate λ (i.e., number of patches per unit area). Thus, in an area A the centers of λA disks were randomly placed (Fig. 1). The radius of each circular region was sampled from an exponential distribution with a mean of 1 m, similar to results from Oleson and Sand-Jensen [34]. Overlaps between circular regions were allowed, creating larger meadows. Two approaches were used to generate heterogeneous 250 m by 250 m seagrass landscapes. First, circular patches were randomly placed on a bare landscape; each circular patch was assumed to be a seagrass meadow represented as a collection of homogenous spaced cylinders with a "shoot density" of 500 shoots/m^2 ("patch scattering scenario"). Second, starting from a landscape assumed to be a continuous homogenous meadow with a shoot density of 500 shoots/m^2, circular gaps were randomly generated; each gap was considered as a disturbance that completely removed all seagrass from the circular region ("gap scattering scenario"). In order to facilitate comparisons across each landscape realization, $R(\lambda)$, with differing patch and gap sizes, the actual cover, $a_{\text{cover}}(\lambda)$, of seagrass on the landscape was calculated as the fraction of the surface covered by seagrass. Each landscape realization allowed for calculation of hourly combined wave-current shear stresses across the landscape. These shear stresses were then used to estimate hourly values of suspended sediment concentrations and light conditions at the top of the canopy or the seafloor if the landscape is completely bare.

Thus for a single landscape realization, $R(\lambda)$, with corresponding actual cover, $a_{\text{cover}}(\lambda)$ and mean water depth, H (m); hourly time series of winds (m/s), photosynthetically active radiation, PAR (μmol/m^2/s), tides (m) and currents (m/s), and water temperature(°C) for the year 2002 (subset of drivers shown in Fig. 2), were used to construct cumulative distribution functions (cdf's) of 1) shear stress on the surface (Pa), 2) suspended sediment concentration SSC (mg/l), and 3) the irradiance in PAR (μmol/m^2/s) reaching the top of the canopy. For each average patch density λ, two realizations were generated and their respective cdf's averaged. Subsequent modification of λ (i.e., number of patches (or gaps) per unit area), and H, for multiple $R(\lambda)$, allowed for exploration of how landscape structure (expressed as a function of λ) and water depth affect the average cdf's of surface shear stresses and the consequent sediment and light environment. The model was run for the year 2002, with an hourly time step for mean water depths ranging from 1 to 4 m MSL, actual landscape cover from 0 to 1, with two realizations for each λ, for both patch and gap scattering perspectives. Each 250 m by 250 m landscape realization was gridded in 0.5 m increments with shear stress, sediment, and light calculated for all 250,000 grid points with a periodic boundary condition. In this manner each 250 m by 250 m landscape realization represents an infinite landscape. Thus, due to the total number of realizations, a quasi-analytical approach was used to estimate the vegetation-modified hydrodynamics, shear stress, sediment and light environment at each grid point allowing for realistic computational times.

2.2. Habitat suitability

Zostera marina is a species requiring a high level of light, roughly 20% of the water surface irradiance for survival [2]. When the light environment is described in terms daily hours of light saturated conditions [4,5] which are temperature dependent [35], roughly 3–5 h [36] are required. In this study, we define habitat suitability in terms of water depths and actual landscape covers, where the spatiotemporal average daily hours of saturation, $\overline{H_{\text{sat}}}$ exceeds 3–5 h. It is important to note that measurements of the hours of saturated conditions required is quite variable [6,37]. Photosynthetic saturation was calculated directly following Zharova et al. [38]

$$I_K = I_{K20}\theta_K^{T-20} \tag{1}$$

where I_{K20} is the saturation irradiance value at 20 °C set to 25.5 mol/m^2 per day [39] and θ_K is a shape value which controls the impact of temperature on saturation and is set to 1.04 [40]. Light reaching the canopy is then calculated as a function of water column light attenuation given hourly records of photosynthetically active radiation (PAR) at the water surface, I_0 (μmol m^2/s). Using the Lambert-Beer law, and a light attenuation coefficient, K_d (m^{-1}) we calculate PAR reaching the seagrass canopy, I_{canopy} (μmol/m^2/s), under hourly

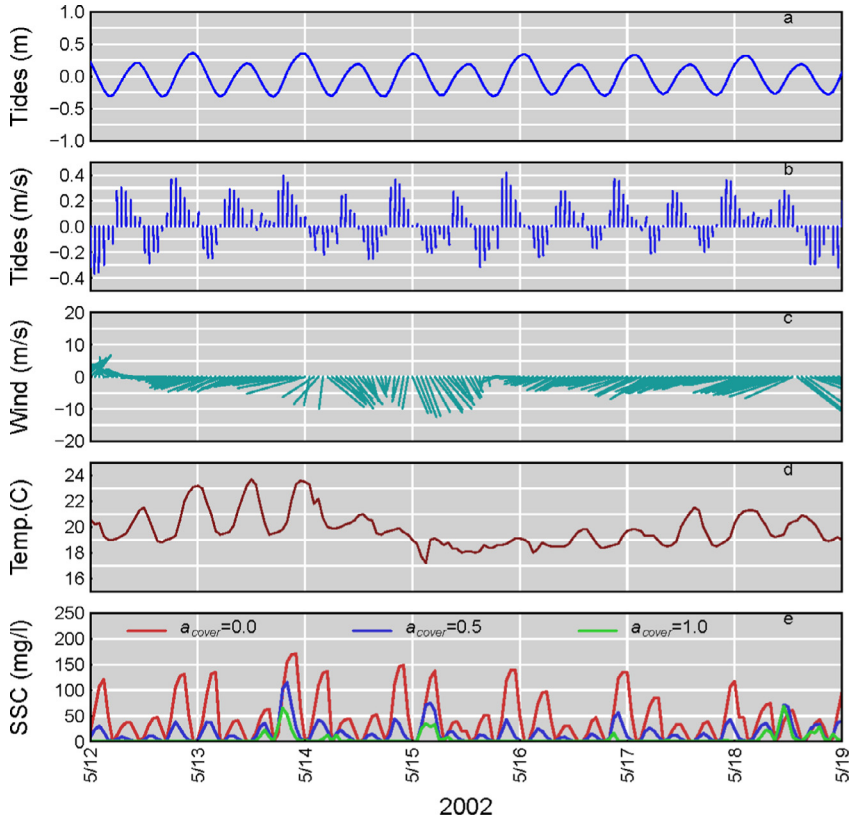

Fig. 2. Time series of tidal elevation(m) (a), tidal current speed and direction (m/s) (b), wind speed and direction (m/s) (c), water temperature (C) (d), and the resultant suspended sediment concentration (mg/l) for bare, half cover and full cover landscapes for a week in May 2002.

tidal, tidal current, wave, and seagrass conditions

$$I_{\text{canopy}} = I_0 e^{-K_d(H-h_c)} \tag{2}$$

where H is the hourly water depth, and h_c (m) is the height of the deflected seagrass canopy.

Light attenuation coefficients are site dependent [41], and a site specific empirical relationship relating SSC (mg/L), concentrations of phytoplankton (*chl a*), and colored dissolved organic matter (*CDOM*) to a light attenuation coefficient was used [1,42].

$$K_d = 0.052SSC + chl\ a \times 0.0154 + CDOM \times 0.28 + 0.0384 \tag{3}$$

We assume non-varying minimal values of *chl a* =5 mg/m^3 and *CDOM* = 0.4 corresponding to the low nutrient environment associated with Hog Island Bay (VCR LTER data base, www1.vcrlter.virginia.edu/home1/?q=data_wq).

2.3. Environmental drivers

While the subsequent general model formulation is applicable to a broad array of locations, the limitations on modeling the light environment require coupled site specific hourly inputs for tidal elevation, current speed and direction, wind speed and direction, PAR and water temperature. Here we used corresponding data records from the coastal bays of the Virginia Coast Reserve Long Term Ecological Research(VCR LTER) site located on the Atlantic side of the Delmarva Peninsula (VCR LTER 37°25′N, 75°46′W) and focus on Hog Island Bay, a shallow coastal bay with half the bay less than a meter deep at mean low water and 1.2 m tidal range [43]. During the 1930s the seagrasses (*Z. marina*) of the VCR LTER coastal bays under duress by disease became locally extinct due to a hurricane [44]. Small natural patches of seagrass were found in the late 1990s and restoration efforts were initiated. Seagrass now covers 1700 ha in the VCR coastal bays [45] from 0.6 m to 1.6 m depths relative to mean sea level (MSL) [46]. Detailed one dimensional models [17,18] predict the emergence of seagrass bistability at depth greater than 1.6 m MSL and provide benchmarks for performance of this model. We utilized hourly tidal currents, wind speed and direction, and water temperature from the year 2002 from the NOAA Wachapreague station, Virginia (WAHV2, 37°36′24″N, 75°41′12″W) with VCR-LTER flux tower at Fowling Point (37 °24′N, 75 °50′W) providing PAR (Fig. 2). Wave generating winds are predominantly from the SSE, SSW and N [47]. Significant wave heights range from 0.06 to 0.08 m with periods 0.6–0.8 s in the summer and 0.12–0.14 m with periods 0.8–1.0 s in the fall [1]. Tidal currents alone are typcially not enough to produce resuspension of sediment and wind- waves are the dominant source of resuspension of the fine sand to silt [48].

2.4. Velocity and shear stress estimates over bare sediment and within meadows

For an average tidal current on the landscape, over bare sediment regions, the vertical velocity profile is expected to be logarithmic, consistent with the classic boundary layer theories for flows parallel to a flat surface with a shear velocity $u_{*,\text{bare}}$ (m/s). Following Lawson et al. [1], the shear stress acting on the seafloor can be calculated as

$$\tau_{b\text{current}} = \rho C_d \overline{U_{\text{curr}}}^{\,2} = \rho u_{*,\text{bare}}^2 \tag{4}$$

where $\overline{U_{\text{curr}}}$ (m/s) is the average velocity of the tidal current, ρ is the water density, g the gravitational acceleration, $C_d = \frac{gn^2}{H^{1/3}}$ is the drag coefficient, g (m/s^2) is gravitational acceleration, H (m) is water depth, and the Manning's roughness coefficient is determined as

$$n = \left[\frac{2\sqrt{8g}}{H^{1/6}} \log_{10}\left(\frac{H}{D_{84}}\right) + 1 \right]^{-1} \tag{5}$$

where D_{84} (m) is the 84th percentile grain size diameter of the bed sediment following [49].

We approximate the shear stress acting on the bed within a seagrass patch by estimating a within canopy velocity. Assuming the same average tidal current condition on the landscape $\overline{U_{\text{curr}}}$, and flow depth H, the vertical velocity within a meadow is significantly modified by a dense (>250 shoots/m^2) seagrass patch. The average velocity on the landscape, $\overline{U_{\text{curr}}}$, can be vertically partitioned into the average velocity within the canopy, $\overline{U_{\text{can}}}$ (m/s), and the average current above the canopy, $\overline{U_{\text{above}}}$ (m/s) (Fig. S1), with both velocities dependent on a variable canopy height h_c, following [50] via an iterative process. We first approximate a surface slope, $S = \tau_{b\text{current}}/\rho g H$, with the shear stress calculated from Eq. (4). Assuming no lateral diversion of flow and starting with a slight increase in the average flow velocity above the canopy we initialize $\overline{U_{\text{above}}} = 1.01\overline{U_{\text{curr}}}$, and subsequent estimates of the above and within canopy average velocities can be iteratively calculated until convergence by

$$\overline{U_{can}} = \sqrt{\left(\frac{2gh_cS + C_v\overline{U_{\text{curr}}}^2}{C_{d\text{veg}}ah_c + C_f}\right)}, \tag{6}$$

$$\overline{U_{\text{above}}} = \left(\frac{H\overline{U_{\text{curr}}} - h_c\overline{U_{\text{can}}}}{H - h_c}\right), \tag{7}$$

where C_v, $C_{d,v}$ and C_f are the drag at the vegetation interface, the drag of the vegetation, and the drag of the bed respectively and $a = Nb$ is the frontal area per unit volume (m^{-1}) and describes the lateral blockage per unit length and is inversely proportional to the adjustment length scale of the flow [51].

Following [50], the deflected canopy height is a function of leaf characteristics, length l (m), thickness, t_h (m), width b (m), tissue density ρ_v (kg/m^3), modulus of elasticity E (Pa), and second moment of area $I_a = bt_h{}^3/12$ (m^4) and can be calculated as

$$h_c = l\left(\frac{1 - \left(1 - 0.9Ca^{-1/3}\right)}{\left(1 + (8 + B^{1.5})Ca^{-1.5}\right)}\right) \tag{8}$$

given the Cauchy number Ca and the buoyancy parameter B.

$$Ca = \frac{(0.5\rho C_{d,\text{flatplate}}bl^3\overline{U_{\text{can}}}^2)}{EI_a} \tag{9}$$

$$B = \left(\frac{(\rho - \rho_v)gbt_hl^3}{EI_a}\right) \tag{10}$$

Iteration of Eqs. (6)–(10) converge to estimates of $\overline{U_{can}}$, $\overline{U_{above}}$, and h_c.

The shear in the velocity profile is then defined as $\Delta U = \overline{U_{\text{above}}} - \overline{U_{\text{can}}}$ and following Eq. (4), the shear stress (Pa) acting on the seafloor within the meadow is estimated as

$$\tau_{b\text{current},veg} = \rho C_d\overline{U_{\text{can}}}^2 \tag{16}$$

It should be reiterated that this approach neglects all lateral diversion of flow. Parameters values in Eqs. (6)–(10) can be found in Table 1. For simplification and numerical efficiency we assume all seagrass patches on the landscape possess a shoot density of 500 shoots/m^2 each with two leaves providing a collection of 1000 leaves/m^2 with constant leaf morphology.

2.5. Shear determination

A landscape in the model is comprised of patches of meadows and bare areas with the properly associated bed shear stresses for any given current condition. However, there are two regions where shear stresses differ. First, the zone in which shear stresses initially reduce to within meadow values, and second a meadow imparts an area of shelter in the region lying behind each meadow based on flow direction. At the upstream edge shear stresses rapidly adjust with significant change within 0.5 m [51,52] At this edge the shear stress at the meadow edge to be equal to shear stress of the adjacent upstream node, and the shear stress one node into the meadow is assumed to equal to the within meadow shear stress. The region lying downstream of the meadow, while barren of seagrass, exhibits reduced shear stresses until boundary layer reformation occurs. Following Markfort [53], Walker [54] and Folkard [55] we assume the length of the reduced shear region to be roughly 30 times the canopy height of the meadow. Within this region the shear velocity is assumed to recover exponentially from $u_{*,\text{veg}}$ to $u_{*,\text{bare}}$ over this distance following Okin [56]. As such the recovery of shear stresses can be estimated as

$$\tau_{b\text{current},x}(x, h_c) = \rho\left[u_{*,\text{bare}} - (u_{*,\text{bare}} - u_{*,\text{veg}})(e^{-kx/h_c})\right]^2 \tag{17}$$

where x is the downstream distance from the meadow.

The parameter k is calculated assuming 99% recovery from the vegetated shear velocity to the bare sediment shear velocity 30 canopy heights, h_c, downstream (Fig. 3a).

$$k = \frac{1}{30}\ln\left(\frac{0.01u_{*,\text{bare}}}{u_{*,\text{bare}} - u_{*,\text{veg}}}\right) \tag{18}$$

As the canopy height is variable, the distribution of tidal current shear stresses on the surface becomes a function of downstream gap size distances in terms of meadow height, similar to Okin [56], but here also depends on tidal flow direction and speed. For each flow direction, speed and subsequent canopy height, gap distances are calculated along a transect aligned with the flow. Shear stresses at every point along a transect can be calculated from the vegetated-patch

Table 1
Key model variables and parameters, descriptions and values.

Variable/parameter	Description and value
b	Blade width set to 0.008 m
c_a	Reference concentration near the bed at height z_a
$C_{d,\text{flatplate}}$	Drag of a flat plate set to 1.95
$C_{d,v}$	Drag for the meadow ~1
C_v	Drag at interface set to 0.04
d	Displacement height for above canopy flow
E	Modulus of elasticity set to 1.4 GPa
H	Water depth (m)
h_c	Deflected canopy height (m)
I_a	Second moment of area (m^4)
I_0	Surface irradiance in PAR (μmol/m^2)
I_{canopy}	Irradiance in PAR (μmol/m^2) at the deflected canopy height
K_d	Light attenuation coefficient (m^{-1})
$K_{\log}(z)$	Vertical diffusivity above the shear layer (m^2/s)
$K_{\text{shear}}(z)$	Vertical diffusivity in the shear layer (m^2/s)
l	Blade length set to 0.4 m
N	Shoot density, here set to 500 shoots/m^2
N_{hs}	Half saturation constant for wave attenuation set to 1500 shoots/m^2
ρ_v	Seagrass density set to 700 km/m^3
T	Temperature (°C)
τ_b	Shear stress applied to the sediment surface (Pa)
τ_{cr}	Critical shear stress for erosion set to 0.04 Pa
t_h	Blade thickness set to 0.00035 m
t_{ml}	Thickness of the shear layer (m)
$\overline{U_{\text{above}}}$	Average tidal velocity above the canopy (m/s)
$\overline{U_{can}}$	Average tidal velocity within the canopy (m/s)
$\overline{U_{curr}}$	Average tidal current velocity (m/s)
ΔU	Shear in the velocity profile (m/s)
u_{dep}	depositional velocity (m/s)
u_*	Bare area shear velocity (m/s)
u_{*n}	Above canopy shear velocity (m/s)
$u_{*,\text{veg}}$	Vegetated area shear velocity (m/s)
w_s	Settling velocity (m/s)
z_i	Height (m) where $K_{\log}(z) = K_{\text{shear}}(z)$

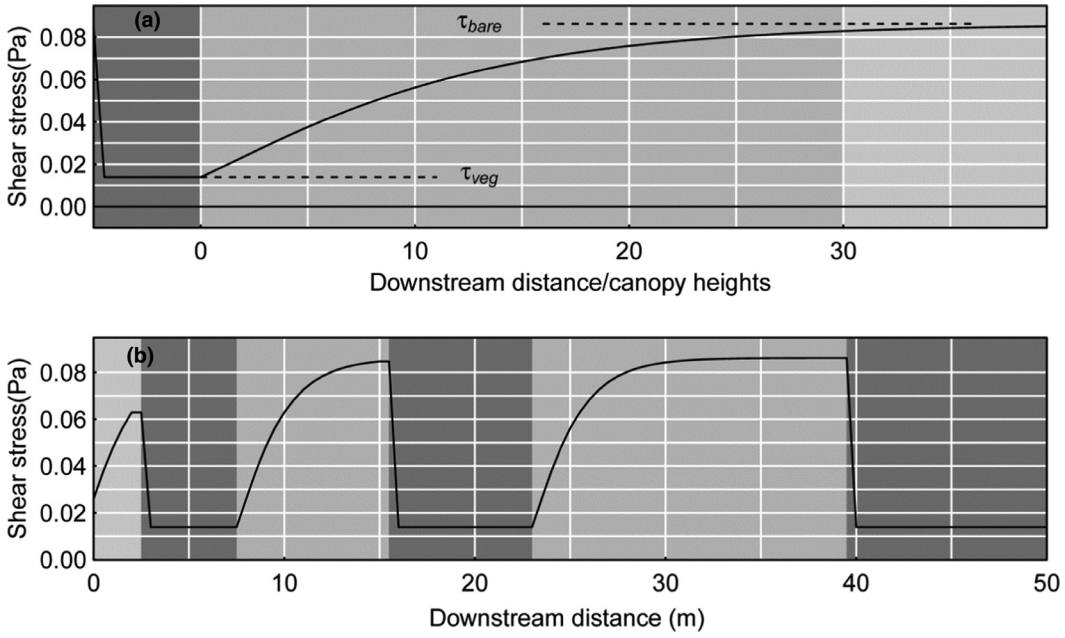

Fig. 3. (a) The penetration of shear stress 0.5 m into a meadow and the sheltering effect of a meadow in the downstream direction. Recovery to 99% of the bare shear velocity occurs at 30 canopy heights downstream. Shear stresses here are those generated by a 0.24 m/s tidal current acting on the landscape with depth 1.5 m MSL with recovery modeled by Eq. (17). (b) The sheltering effect of multiple meadows in the downstream direction along a transect across the landscape. Vegetated sections exhibit minimum shear stress (dark gray region) increasing shear stress in the sheltered regions (gray) until boundary layer reformation has occurred.

and bare-sediment shear stresses produced by a given tidal current (Eqs. (4), (16)), in combination with Eq. (17) (Fig. 3b). This is performed for equally spaced transects every 0.5 m across the landscape for a given flow direction.

2.6. Waves

Wave shear stress is determined from significant wave height, H_{sig} (m), water depth, H, wavelength, L (m), and period, T (s), generated from the fetch-limited shallow water wave model of Young and Verhagen [57] as

$$\tau_{bwave} = \rho\left(\frac{f}{2}\right){U_b}^2 \tag{19}$$

where the depth dependent wave orbital velocity, U_b, at the bed is given by

$$U_b = \frac{\pi H_{sig}}{T \sinh(2\pi H/L)} \tag{20}$$

while the friction factor, f, is calculated following Lawson et al. [1]. Wave attenuation and wave energy dissipation due to a submerged canopies is complex [58–62], depending not only on distance a wave propagates over a meadow, but also on meadow geometry, and vegetation characteristics. However, the impact of seagrass on near bed orbitals for 1–2 s wind waves, typical of this study site [1], is small [62]. For simplicity, we simply by reducing the wave orbital velocity assuming a Monod equation, $U_{bmeadow} = U_b(\frac{N_{hs}}{N+N_{hs}})$, with half saturation constant, N_{hs} of 1500 shoots/m^2 following van der Heide [63]. With the constant shoot density, N=500 shoots/m^2, a 25% reduction of near bed wave orbital velocities is obtained, similar to site measurements from the VCR [64]. Wave attenuation of near bed orbitals is only performed over the landscape where seagrass is present. The combined effect of waves and currents on total bed shear stress is calculated as

$$\tau_b = \sqrt[2]{{\tau_{bwave}}^2 + {\tau_{bcurrent}}^2} \tag{21}$$

following [65].

The effective cover of a landscape can be estimated by rescaling these combined hourly shear stresses between 0 (minimum shear stress on the landscape) and 1 (maximum shear stress on the landscape) for each hour, and taking the temporal average at each grid location. This also allows for examining the impact of actual cover of the landscape on the relative shear stress environment (Fig. 4).

2.7. Sediment resuspension

In order to characterize the light environment, calculation of suspended sediment concentrations is required. In areas without seagrass roughness elements (e.g., bare sediment), a Rouse profile [66], a steady state analytical solution of the one dimensional advection diffusion equation assuming a parabolic eddy diffusivity, is used

$$c_s(z) = c_a\left[\frac{z(H-z_a)}{z_a(H-z)}\right]^{-\frac{w_s}{\kappa u_*}} \tag{22}$$

where u_* is the shear velocity, w_s (m/s) is the settling velocity, and c_a (mg/L) is the reference concentration for suspended sediments near the bed at height z_a.

Turbulent mixing above the patches of seagrass is more complicated. The mixing within and above the canopy can be dominated by shear scale vortices and the diffusivity of this region scales with the thickness of the shear layer t_{ml} (m), and the shear, ΔU [21]. Using the dimensionless results from Ghisalberti and Nepf [21] we note that the top of the shear layer corresponds to roughly two and a half times the canopy height with the maximum diffusivity (m^2/s) occurring halfway through the shear layer and we assume the shear layer begins at the bed. This can be simply modeled as a parabolic diffusivity which has a maximum of $0.0125 t_{ml}\Delta U$ at the height $t_{ml}/2$.

$$K_{shear}(z) = -0.05\Delta U\, z\left(\frac{z}{t_{ml}} - 1\right) \tag{23}$$

To estimate mixing above the shear layer we assume the velocity profile above the canopy follows a logarithmic profile with the velocity at the top of the canopy equal to $\overline{U_{can}}$ a shear velocity u_{*n}, and displacement height, d (m), and the von Karman constant κ. For this layer, the

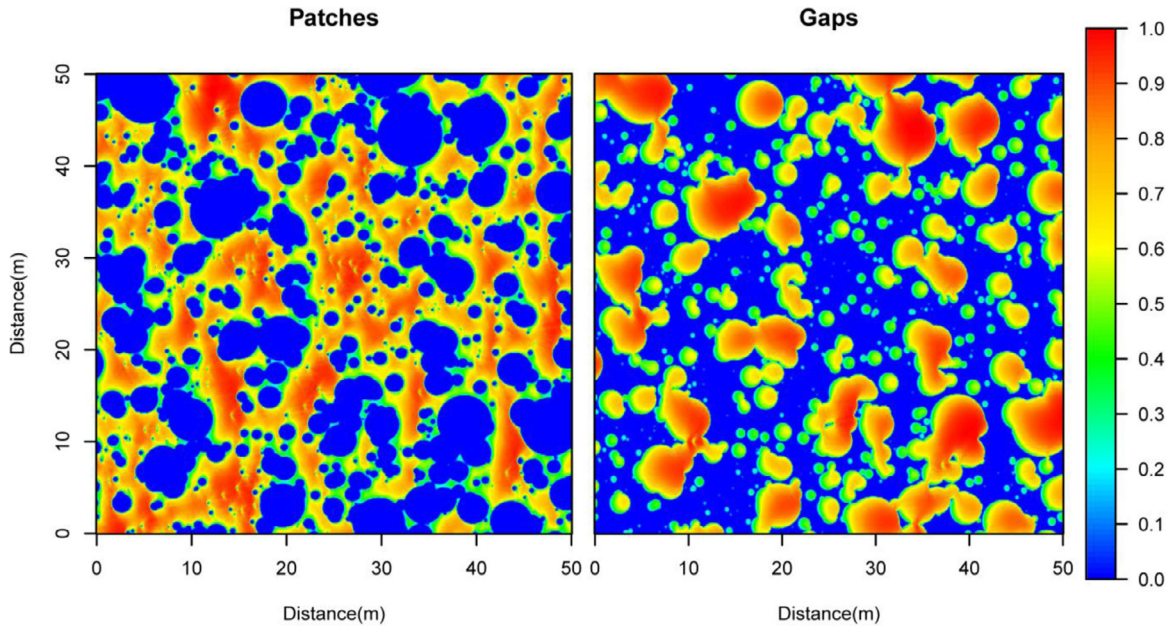

Fig. 4. Dimensionless scaled shear stresses for all hourly wave and current conditions of 2002 with mean water depth of 1.5 m MSL. Two 50 m by 50 m sub regions of the 250 m by 250 m landscape are shown with identical distribution of disks and actual cover $a_{cover} = 0.5$, $R(0.1125\ m^{-2})$. The regions are shown from the both perspective of randomly scattering circular seagrass patches or circular gaps within a homogenous seagrass meadow.

parabolic eddy diffusivity, K_{log} (m^2/s) can be calculated as

$$K_{log}(z) = \kappa u_{*n}(z-d)\left(1 - \frac{(z-d)}{(H-d)}\right), \tag{24}$$

Given

$$u_{*n} = \frac{\kappa \Delta U}{\ln(Z - d/e(h_c - d))} \tag{25}$$

In this manner, the vertical diffusivity from the bottom of the shear layer to the top of the water column can be considered as a piecewise curve. From the reference concentration height z_a to height z_i the diffusivity is modeled as in Eq. (23), and from z_i to H the diffusivity is modeled as in Eq. (24). The height z_i, lying between z_a and H, is the height at which the diffusivity profiles given by Eqs. (23) and (24) intersect.

$$z_i = \frac{0.05\Delta U t_{ml} - \kappa u_{*n} + \frac{2d\kappa u_{*n}}{d-H} \pm \sqrt{D}}{0.1\Delta U + \frac{\kappa u_{*n}}{d-H}}. \tag{26a}$$

where

$$D = -4d\left(-1 + \frac{d}{d-H}\right)\kappa u_{*n}\left(0.05\Delta U + \frac{\kappa u_{*n}}{d-H}\right) + \left(-0.05\Delta U t_{ml} + \kappa u_{*n} - \frac{2d\kappa u_{*n}}{d-H}\right)^2, \tag{26b}$$

Assuming steady state and integrating the one dimensional advection diffusion equation we find that the downward settling is equal to the upward mixing due to the diffusivity.

$$-w_s c_s = K\frac{dc_s}{dz} \tag{27}$$

Integration of Eq. (27) using Eqs. (23) and (24) leads to a piecewise modified Rouse profile, where the mixing within the shear layer scales with ΔU and the mixing in the logarithmic layer scales with the appropriate shear velocity, u_{*n}.

$$c_s(z) = \begin{cases} c_a\left[\frac{z(t_{ml}-z)}{z_a(t_{ml}-z_a)}\right]^{-\frac{20w_s}{\Delta U}} & z_a \le z \le z_i \\ c_{a2}\left[\frac{(z-d_0)(H-z_i)}{(H-z)(z_i-d_0)}\right]^{-\frac{w_s}{\kappa u_{*n}}} & z_i < z < H \end{cases} \tag{28}$$

The reference suspended sediment concentration, c_a drives the lower profile, while the upper reference concentration, c_{a2} is related to c_a as

$$c_{a2} = c_a\left[\frac{z_i}{(t_{ml}-z_i)}\right]^{-\frac{20w_s}{\Delta U}} \tag{29}$$

The reference concentration is determined based on excess shear stress [1,67], but also includes an active bed layer determined by shear stress [65], for a bed comprised of three grain size classes, 40% Sand (125 μm), 50% silt (63 μm), and 10% clay (32 μm). The critical erosion shear stress is set to 0.04 Pa [1]. Integration of Eqs. (22) and (28) for each size class gives SSC based on shear velocity, bed shear, mixing layer thickness, water depth, velocity shear, settling velocity, displacement height and bed sediment concentration.

Applicability of Eqs. (22) and (28) to time-dependent scenarios depends on diffusion time $T_{dif} = H^2/\overline{K}$ (s) and diffusion length scales $L_{dif} = \overline{U}T_{dif}$ (m), which are functions of water height, the vertically averaged diffusivity, and the average current velocity. It is important to note that while the diffusion time scale is typically less than the model time step, the diffusion length scale can be much longer than the distance between bare and covered regions. As such, steady state assumptions in Eqs. (22) and (28) are only fully met for the full covered and bare landscapes and will likely result in overestimates of SSC [68,69] for mid ranges of landscape cover at high flow velocities and underestimates at low flow velocities. To remedy the applicability of steady state solutions to low flow velocities, maintenance of fine grained sediment in suspension as to not underestimate SSC is required. Here, based on a bed load transport Rouse number [66], $\frac{w_s}{\kappa u_{dep}}$=2.5, sediment is allowed to remain in suspension until the depositional velocity, u_{dep}, and settling velocities are equal [70]. Typically the depositional velocity is set equal to the shear velocity. Here due to combined wave and current shear stresses we calculate the depositional velocity as $u_{dep} = \sqrt{\frac{\tau_b}{\rho}}$.

As such, meadows and the protected region behind the meadow become deposition favoring environments in comparison to the bare sediment areas. As the velocity changes direction the duration of time when the deposition favoring conditions are met allows for

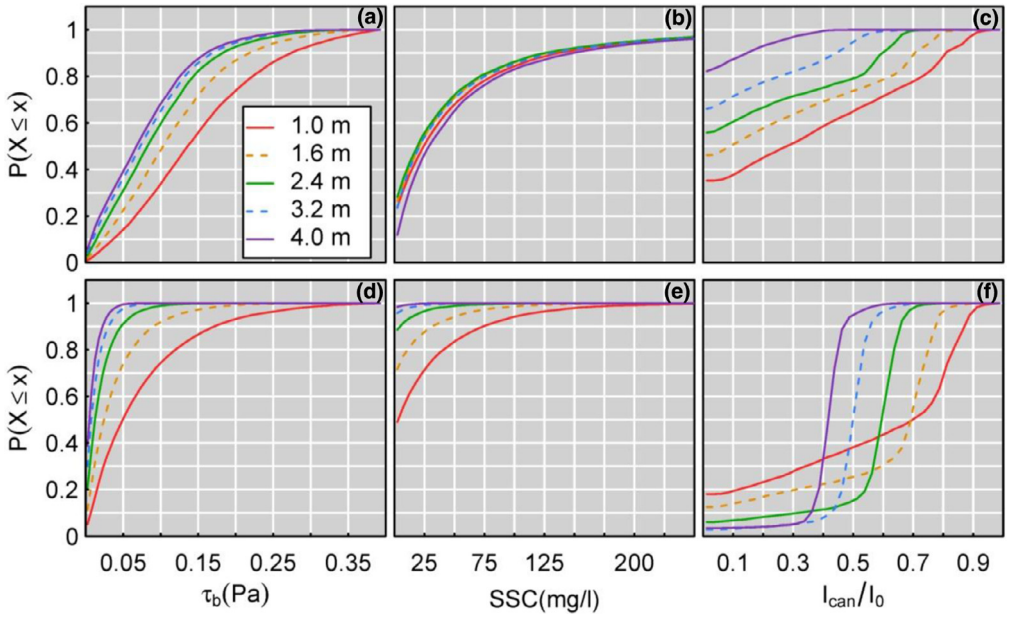

Fig. 5. Cumulative distributions of bottom shear stress (a, d), suspended sediment concentration (b, e), and fraction of incident light reaching the deflected canopy height (c, f), for bare landscapes (a, b, c) and full cover landscapes (d, e, f) at various water depths relative to MSL.

calculation of a partial flux of sediment in each size class out of the water column based on settling velocity for each grid location.

Advection of sediment in the flow direction is incorporated as linear weighted average. Each node on the grid exhibits the sediment concentration of the nodes some distance upstream. This distance is a function of average current, settling velocity and water depth or time step length.

$$d_{\text{advect}} = \overline{U_{\text{curr}}}\left(\min[\frac{H}{w_s}, \Delta t]\right) \tag{30}$$

Weights are determined linearly based on the advective distance and the number of nodes upstream involved in the average. As the boundary of the landscape is periodic, SSC is advected out one boundary and into the boundary opposite and lateral dispersion is not allowed.

3. Results

The full and bare cover, $a_{\text{cover}} = 1$ and 0 respectively, represent the two extremes in terms of the light and sediment environment. For a bare landscape examining the cdf's of shear stress, SSC and fraction of daylight reaching the deflected canopy height (the seafloor for bare landscapes) at various depths revealed that while bed shear stresses diminish with depth (Fig. 5a), SSC remained relatively constant across the water depths modeled (Fig. 5b). The resultant cdf's of fraction of daylight reaching the canopy predict a steady decline in the light environment (Fig. 5c). In contrast, the cdf's of shear stress for a full cover landscape (Fig. 5d) predict the significant reduction in shear stresses caused by the presence of seagrass, with consequent large reductions in suspended sediment concentrations (Fig. 5e). This large reduction in SSC results in initial increases in the light environment from ~1 to 2 m MSL and subsequent decrease in light conditions as depth increases (Fig. 5f).

However, we are defining habitat suitability in terms of $\overline{H_{\text{sat}}}$ which depends also on temperature and seasonality. For the VCR, storms typically arrive from October through April [1]. These fall and winter storms generate higher wind wave shear stresses on the seafloor resulting in increased SSC and reduction in PAR reaching the seafloor. Moreover, due to high temperature limits on seagrass growth in the middle of summer [71,72], there are distinct seasonal and depth variations in $\overline{H_{\text{sat}}}$ for both bare and full cover landscapes (Fig. 6). While

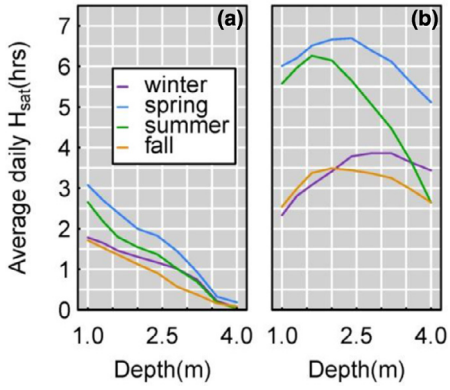

Fig. 6. $\overline{H_{\text{sat}}}$ as a function of water depth and season for: a) a bare sediment landscape $a_{\text{cover}} = 0$, $R(0\ \text{m}^{-2})$ and b) a full cover landscape $a_{\text{cover}} = 1$, $R(1.11\ \text{m}^{-2})$. For a full cover landscape, during all seasons, a depth which maximizes $\overline{H_{\text{sat}}}$ appears. For bare landscape $a_{\text{cover}} = 0$, $R(0\ \text{m}^{-2})$, $\overline{H_{\text{sat}}}$ monotonically declines with depth.

$\overline{H_{\text{sat}}}$ declines with depths for all seasons on a bare landscape, there are distinct maxima which occur at moderate depths under full cover landscapes (Fig. 6b) for all seasons, but these optima are more apparent for spring and summer and exist due to the combined depth effects on light attenuation and waves.

Wave shear stress is a function of near bed orbital velocity, which diminishes with increasing water depth (Eq. (20)). As depth increases, wave generated sediment resuspension declines. However, as depth increases, light must also penetrate further to reach the canopy or seafloor. As a result, once water depths increase above a certain value, the improvement in the light environment associated with declining wave orbitals and reduced sediment resuspension is no longer able to offset the light loss due to the presence of a deeper water column. In this manner, the combined effects of sediment resuspension and water column depth result in an increase in light availability initially with increasing depth and then a decline in deeper waters. In addition, to the effects of water depth on light and wave orbitals, the presence of seagrass also leads to reduced wave-generated bed shear stress. When the sediment bed is fully covered by vegetation,

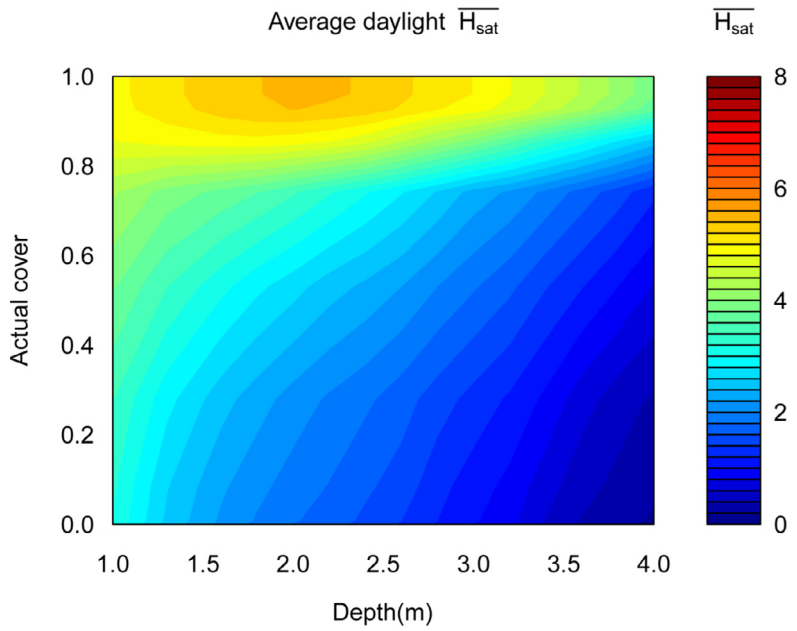

Fig. 7. $\overline{H_{sat}}$ as a function of water depth and actual cover. There is an optimum region between 1.4 and 2.4 m MSL at large actual covers. At low covers $\overline{H_{sat}}$ is not large enough (>3–5 h) to promote seagrass growth.

light availability to the canopy generally improves initially with water depth (Fig. 7f). Eventually, with the significant decrease in wave bed shear stress with depth, resuspension becomes negligible, and the cdf's of light reflect the dependence of the light environment on tidal elevation (Fig. 5f).

The importance of this dual role of depth on the light environment and subsequent average daily hours of saturation depends on the actual cover on the landscape (Fig. 7). Assuming *Z. marina* requires a daily threshold value of roughly 3–5 h of saturation [5,6] the model predicts alternate states depending on actual cover and water depth. For all depths modeled for 2002, landscapes generated from the patch building perspective with $a_{cover} < 0.4$ fall below this habitat threshold and any seagrass meadows on these landscapes could be expected to decline due to poor light habitat. As depth increases, even a more fully covered landscape is unable to promote an adequate light habitat. As such, there is a threshold that is depth and actual cover-dependent, above which the light habitat would favor growth and maintenance of seagrass. Thus, for the depth ranges and actual covers modeled, we predict emergence of alternate state dynamics. Moreover, there exists an optimal environment in terms of $\overline{H_{sat}}$ (Fig. 7) at moderate depths and high actual covers. The depth range for this optimal environment at high actual cover corresponds to an inadequate light environment at low actual cover (e.g. for initial seagrass establishment) (Fig. 7).

4. Discussion

This paper investigated how vegetated patches influence a larger area than their footprint, including an adjacent downstream area, which directly impacts the shear stress distribution on the landscape and the subsequent suspended sediment and light environment. This effective cover, e_{cover}, due to the presence of this sheltered region (Fig. 8) can be calculated from the spatiotemporal averaged scaled shear stress acting on the landscape across various actual covers, a_{cover} (Fig. 4). From the patch scattering perspective, for $a_{cover} = 0.5$, $R(0.11\ m^{-2})$, the $e_{cover} = 0.645$. Similarly, at $a_{cover} = 0.5$, $R(0.11\ m^{-2})$, $e_{cover} = 0.636$ for the circular gap scenario. In general, there exist small geometrical differences between cases in which a given actual cover is attained by (1) randomly scattering patches of meadows or by (2) opening gaps in a uniform seagrass meadow (Fig. 8b). For $a_{cover} = 0.5$, landscapes with circular meadows generated with $R(0.11\ m^{-2})$, exhibit only slightly lower shear stress conditions at the seafloor than landscapes with circular gaps. However, this difference does not affect the light habitat in terms of daily hours of saturation.

Results indicate that it takes around 1000 disturbed areas (gaps) to reduce the effective cover to 90%. For a full cover landscape at 1.5 m MSL, it would take over 10,000 gaps for the landscape to cross over the threshold 3–5 h of $\overline{H_{sat}}$ requirement and fall into the attractive domain of a bare landscape (Figs. 7 and 8a). Alternately, at the same water depth, it would only take roughly 2000 patches to cross from the bare sediment attractive domain into a light environment which would favor further seagrass growth. In contrast at 3.5 m MSL, it would take only 1000 disturbed areas to push the light environment to one not favorable for seagrass, and over 10,000 patches to scaffold a bulk light environment favorable to seagrass (Figs. 7 and 8a). The effective cover from both gap and patch perspectives, are roughly equivalent across actual covers (Fig. 8b). Regardless of perspective, due to ability of an individual patch to affect an area larger than itself, effective cover rather than actual cover may need to be considered when examining the success or failure of restoration efforts as well as the resilience of landscapes with existing cover to disturbances.

These results differ from prior work [23,63] in the sense that the suitable habitat depth range and the prediction of bistability produced here is (1) a function of the total landscape rather than an individual meadow (2) average meadow shoot densities are held constant rather than time and depth varying and (3) SSC are likely overestimated resulting in underestimates of the light environment. This spatial approach allowed for examination of how bare areas and patches of seagrass interact with regards to light and sediment which are neglected in one-dimensional models.

As a result of allowing for advection of sediment, bed grain size distributions and resuspension mechanisms ultimately both play important roles in determining the transport and light environment. For a situation where resuspension is strongly affected by fauna [73,74] the reduction of shear stresses by the presence of seagrass may have little impact on the bulk light environment. Even focusing on situations where resuspension is dominated by wave current shear stresses, prior work has predicted the collapse of the positive feedback between seagrass and their light environment when the bed grain size distribution coarsens [23]. In a sandy substrate

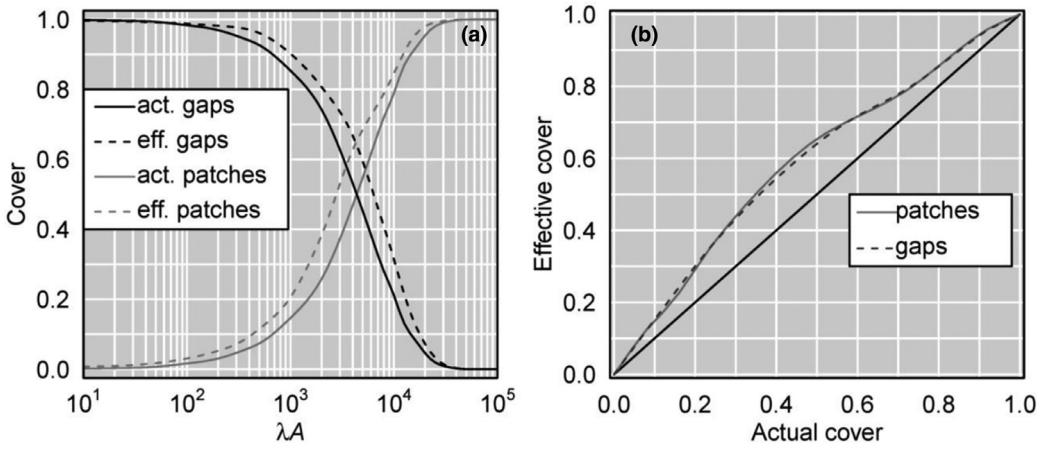

Fig. 8. A. Actual (solid) and effective cover (dashed) as a function of λA (number of disks) and the perspectives of adding patches (increases with λA) or removing gaps (decreases with λA). B. Effective cover as a function of actual cover for meadow and disturbance scenarios. The difference between effective and actual cover is maximized between actual covers of 0.4 and 0.6.

environment, the positive feedback between vegetation and light is likely to be negligible because of the paucity of sediment in suspension. As the seafloor sediment distribution increases in silt and clay content, this positive feedback becomes important and alternate state dynamics can emerge. The slow settling velocity and consequent large advective distance of fine grained sediment indicates the light environment is less likely to be locally controlled. As such a landscape scale approach to estimating habitat suitability may be more appropriate. In contrast, as grains size distributions coarsen, suspended sediment control shifts toward a more localized region. Thus, depending on the grain size distribution of the seafloor, this concept of effective cover may need to be considered. This is especially important for constraining suitable habitat when identifying suitable restoration locations.

The emergence of bistable dynamics has significant consequences in that a system, which undergoes a relatively strong disturbance, can fall into the attraction domain of an alternate state from which it cannot recover [12,15,75]. Such disturbances for seagrass meadows can occur from a variety of causes [31,33,76] and recovery of bare gaps can take years [77]. The results here indicate that even when disturbances open a relatively large number of gaps (e.g., $\lambda A = 10{,}000$) in an initially continuous seagrass meadow, a favorable light environment may still exist because the effective cover is far larger than the actual vegetation cover (Fig. 10a). This indicates that in fine sediment environments where sediment resuspension and light availability limits seagrass growth, carpeted seagrass landscapes are likely more resilient to disturbances which remove actual cover. The results herein also indicate that due to the discrepant rates of light and wave orbital attenuation as water depth increases, an optimum light environment develops. This optimum varies seasonally (Fig. 6b) and occurs in depth ranges where the light conditions predicted for a bare landscape would inhibit the initial establishment of seagrass meadows (Fig. 6a). A pre-existing full cover seagrass landscape within this depth range is relatively resilient to gap causing disturbances. However, with enough disturbances, the landscape cover could pass a threshold value for fractional cover from which the general light environment no longer favors growth, and the original full cover landscape is unable to be recovered.

The modeling approach makes several assumptions and simplifications in modification tidal currents and waves by seagrass, as well as sediment resuspension in order to leverage multiple simulations at varying densities and depths on a landscape. First, meadows were assumed to be composed of time invariant characteristics (Table 1), whereas the canopy structure of seagrass meadows is temporally variable [18,40]. Second, horizontal diversion of the flow around meadows was not included [51,78] and the modeling approach assumes depth averaged velocities over bare and vegetated areas to be equal, likely overestimating within-meadow velocities and shear stresses, and underestimating the same in lateral adjacent bare regions. Third, the wave energy dissipates with distance over submerged canopies [60,79,80], interacts with currents [81–83], and the simplified approach herein neglects any lateral effect along the direction of wave propagation. It is important to note that even though this lateral effect is neglected, the impact of seagrass canopies on near bed orbital for short period waves is small [62]. Lastly, the application of steady state solutions suspended sediment profiles is not well adapted to heterogeneous landscapes where the diffusion length scale is longer than the patch gap distances and will likely tend to overestimate SSC for higher current velocities and underestimate SSC for ebb currents [68,69]. The underestimation of SSC is partly remedied by maintaining fine grained sediment in suspension, as such the model likely overestimates SSC, and underestimates the consequent light environment.

For the simulations herein the minimum modeled patch or gap radius was 0.5 m due to the gridding of the 250 m by 250 m landscape. This corresponds to minimum gap size able to affect the hydrodynamics [26] as well as observed minimum patch sizes [27,29]. Larger radii are representative of larger reseeding areas or disturbances. Thus, the mean radius used in this study is a size from which larger more contiguous meadows or gaps could be generated by multiple overlapping disks in the spatial Poisson process. While prior work involved various landscape metrics [33] including those from percolation theory [26] to set thresholds for actual cover and pattern formation, this study incorporates downstream shear partitioning [56] and an effective shelter area [55] to examine the light environment. Similar to most models, these simplifications do not fully represent the complex processes involved, however these simplifications allowed for the computational ability to fully explore the phase space of actual cover and depth to provide estimates habitat suitability.

Estimates of habitat suitability leverage the concept of hours of saturated light conditions to incorporate the impact of temperature on plant carbon balance. The basic requirement of 3–5 h of saturated conditions [6] may not be indicative of this site and $\overline{H_{sat}}$ requirements have been calculated from as low as 2 h [84] to as high as 12 h [85,86]. CO_2 manipulative experiments seem to indicate a threshold around 4 h [84]. It should be noted that the combined effects of light attenuation and wave orbital attenuation with depth result in a similar light optimum (Fig. S2) when just examining fraction of light reaching the canopy indicating that other light-temperature metrics for habitat suitability are likely to demonstrate similar results.

5. Conclusions

The effective cover due to the presence and distribution of seagrasses on a landscape has important controls on the distributions of shear stress, suspended sediment and consequent light environment across the landscape. For high actual cover landscapes, an optimum light environment emerges within a depth range in which seagrasses possess limited resilience to disturbances due to differential rates of wave orbital and light attenuation with depth. At low fractional cover, light attenuation is primarily controlled by water depth as SSC, and the consequent light attenuation coefficient, remain high across all water depths. This optimum light habitat under high actual cover, occurs in depth ranges where at low actual cover the light habitat is unable to support seagrass. This modeling prediction of alternate state dynamics at a landscape scale suggests that effective cover may need to be considered when planning restoration efforts, delineating habitat, or predicting responses of existing meadows to disturbances. The finding that water depth conditions for optimal seagrass productivity may have an overall low resilience is consistent with findings from other systems (e.g. [87]).

Acknowledgments

Partial support of this study was provided by the Virginia Coast Reserve LTER project, which was supported by National Science Foundation grant DEB-0621014. We would like to thank David Carr for high speed computing and Ilgar Safak for tidal current modeling. We would also like to thank three anonymous reviewers for their insight and guidance.

Joel Carr acknowledges support from the US Geological Survey Climate and Land Use Research and Development program. Any use of trade, product, or firm names is for descriptive purposes only and does not imply endorsement by the U.S. Government.

Supplementary materials

Supplementary material associated with this article can be found, in the online version, at doi:10.1016/j.advwatres.2015.09.001.

References

[1] Lawson SE, Wiberg PL, McGlathery KJ, Fugate DC. Wind-driven sediment suspension controls light availability in a shallow coastal lagoon. Estuaries Coasts 2007;30:102–12. http://dx.doi.org/10.1007/bf02782971.
[2] Duarte CM. Seagrass depth limits. Aquat Bot 1991;40:363–77. http://dx.doi.org/10.1016/0304-3770(91)90081-F.
[3] Dennison WC, Orth RJ, Moore KA, Stevenson JC, Carter V, Kollar S, et al. Assessing water-quality with submersed aquatic vegetation. Bioscience 1993;43:86–94. http://dx.doi.org/10.2307/1311969.
[4] Zimmerman RC, Alberte RS. Light availability, root anoxia and patterns of carbon allocation in the marine angiosperm *Zostera marina* L (eelgrass). Plant Physiol 1995;108:24.
[5] Zimmerman RC, Kohrs DG, Steller DL, Alberte RS. Carbon partitioning in eelgrass-regulation by photosynthesis and the response to daily light-dark cycles. Plant Physiol 1995;108:1665–71. http://dx.doi.org/10.1104/pp.108.4.1665.
[6] Zimmerman RCR, Reguzzoni JLJ, Alberte RS. Eelgrass (*Zostera marina* L.) transplants in San Francisco Bay: role of light availability on metabolism, growth and survival. Aquat Bot 1995;51:67–86. http://dx.doi.org/10.1016/0304-3770(95)00472-c.
[7] De Boer WF. Seagrass–sediment interactions, positive feedbacks and critical thresholds for occurrence: a review. Hydrobiologia 2007;591:5–24. http://dx.doi.org/10.1007/s10750-007-0780-9.
[8] Heiss WM, Smith AM, Probert PK. Influence of the smalt intertidal seagrass *Zostera novazelandica* on linear water flow and sediment texture. N Z J Mar Freshw Res 2000;34:689–94. http://dx.doi.org/10.1080/00288330.2000.9516970.
[9] Gacia E, Duarte CM. Sediment retention by a Mediterranean *Posidonia oceanica* meadow: the balance between deposition and resuspension. Estuar Coast Shelf Sci 2001;52:505–14. http://dx.doi.org/10.1006/ecss.2000.0753.
[10] Gacia E, Duarte CM, Marba N, Terrados J, Kennedy H, Fortes MD, et al. Sediment deposition and production in SE-Asia seagrass meadows. Estuar Coast Shelf Sci 2003;56:909–19. http://dx.doi.org/10.1016/s0272-7714(02)00286-x.
[11] Wilson JB, Agnew ADQ. Positive-feedback switches in plant-communities. Adv Ecol Res 1992;23:263–336. http://dx.doi.org/10.1016/s0065-2504(08)60149-x.
[12] Gunderson LH. Ecological resilience—in theory and application. Annu Rev Ecol Syst 2000;31:425–39. http://dx.doi.org/10.1146/annurev.ecolsys.31.1.425.
[13] Walker B, Holling C, Carpenter S, Kinzig A. Resilience, adaptability and transformability in social–ecological systems. Ecol Soc 2004;9 http://www.ecologyandsociety.org/vol9/iss2/art5/.
[14] Scheffer M, Carpenter S, Foley JA, Folke C, Walker B. Catastrophic shifts in ecosystems. Nature 2001;413:591–6. http://dx.doi.org/10.1038/35098000.
[15] Scheffer M, van Nes EH. Mechanisms for marine regime shifts: can we use lakes as microcosms for oceans? Prog Oceanogr 2004;60:303–19. http://dx.doi.org/10.1016/j.pocean.2004.02.008.
[16] Holling CS. Resilience and stability of ecological systems. Annu Rev Ecol Syst 1973;4:1–23 CR – Copyright © 1973 Annual Reviews]. http://dx.doi.org/10.2307/2096802.
[17] Carr J, Odorico P, McGlathery K, Wiberg P. Modeling the effects of climate change on eelgrass stability and resilience: future scenarios and leading indicators of collapse. Mar Ecol Prog Ser 2012;448:289–301. http://dx.doi.org/10.3354/meps09556.
[18] Carr J, D'Odorico P, McGlathery KJ, Wiberg PL. Stability and resilience of seagrass meadows to seasonal and interannual dynamics and environmental stress. J Geophys Res G Biogeosci 2012;117. http://dx.doi.org/10.1029/2011jg001744.
[19] Abdelrhman MA. Effect of eelgrass *Zostera marina* canopies on flow and transport. Mar Ecol Ser 2003;248:67–83. http://dx.doi.org/10.3354/meps248067.
[20] Abdelrhman MA. Modeling coupling between eelgrass *Zostera marina* and water flow. Mar Ecol Ser 2007;338:81–96. http://dx.doi.org/10.3354/meps338081.
[21] Ghisalberti M, Nepf HM. The limited growth of vegetated shear layers. Water Resour Res 2004;40. http://dx.doi.org/10.1029/2003wr002776.
[22] Ghisalberti M, Nepf H. The structure of the shear layer in flows over rigid and flexible canopies. Environ Fluid Mech 2006;6:277–301. http://dx.doi.org/10.1007/s10652-006-0002-4.
[23] Carr J, D'Odorico P, McGlathery K, Wiberg P. Stability and bistability of seagrass ecosystems in shallow coastal lagoons: role of feedbacks with sediment resuspension and light attenuation. J Geophys Res G Biogeosci 2010;115. http://dx.doi.org/10.1029/2009jg001103.
[24] Chen SN, Sanford LP, Koch EW, Shi F, North EW. A nearshore model to investigate the effects of seagrass bed geometry on wave attenuation and suspended sediment transport. Estuaries Coasts 2007;30:296–310. http://dx.doi.org/10.1007/bf02700172.
[25] Van der Heide T. Spatial self-organized patterning in seagrasses along a depth gradient of an intertidal ecosystem. Ecology 2010;91:362–9. http://dx.doi.org/10.1890/08-1567.1.
[26] Luhar M, Rominger J, Nepf H. Interaction between flow, transport and vegetation spatial structure. Environ Fluid Mech 2008;8:423–39. http://dx.doi.org/10.1007/s10652-008-9080-9.
[27] Olesen B. Patch dynamics of eelgrass *Zostera marina*. Mar Ecol Prog Ser 1994;106:147. http://dx.doi.org/10.3354/meps106147.
[28] Bell SS. Linking restoration and landscape ecology. Restor Ecol 1997;5:318–23. http://dx.doi.org/10.1046/j.1526-100X.1997.00545.x.
[29] Fonseca MS. Influence of physical setting on seagrass landscapes near Beaufort, North Carolina, USA. Mar Ecol Prog Ser 1998;171:109. http://dx.doi.org/10.3354/meps171109.
[30] Fonseca M. Modeling seagrass landscape pattern and associated ecological attributes. Ecol Appl 2002;12:218–37. http://dx.doi.org/10.1890/1051-0761 (2002)012[0218:mslpaa]2.0.co;2.
[31] Fonseca MS. Biomechanical factors contributing to self-organization in seagrass landscapes. J Exp Mar Bio Ecol 2007;340:227. http://dx.doi.org/10.1016/j.jembe.2006.09.015.
[32] Fonseca MS. Factors influencing landscape pattern of the seagrass *Halophila decipiens* in an oceanic setting. Estuar Coast Shelf Sci 2008;76:163. http://dx.doi.org/10.1016/j.ecss.2007.06.014.
[33] Larkum A.W.D., Orth R.J., Duarte C.M., Bell S.S., Fonseca M.S., Stafford N.B. Seagrass ecology: new contributions from a landscape perspective, Springer, Netherlands; 2006, p. 625–645.
[34] Olesen B, Sand-Jensen K. Biomass-density patterns in the temperate seagrass *Zostera marina*. Mar Ecol Prog Ser 1994;109:283–91. http://dx.doi.org/10.3354/meps111283.
[35] Moore K, EC S, DB P, RJ O. Eelgrass survival in two contrasting systems: role of turbidity and summer water temperatures. Mar Ecol Prog Ser 2012;448:247–58. http://dx.doi.org/10.3354/meps09578.
[36] Zimmerman R, Reguzzoni J. Assessment of environmental suitability for growth of *Zostera marina* L.(eelgrass) in San Francisco Bay. Aquat Bot 1991;39:353–66. http://dx.doi.org/10.1016/0304-3770(91)90009-t.
[37] Dennison W, Alberte R. Role of daily light period in the depth distribution of *Zostera marina* (eelgrass). Mar Ecol Prog Ser 1985;25:51–61. http://dx.doi.org/10.3354/meps025051.
[38] Zharova N, Sfriso A, Voinov A, Pavoni B. A simulation model for the annual fluctuation of *Zostera marina* biomass in the Venice lagoon. Aquat Bot 2001;70:135–50. http://dx.doi.org/10.1016/s0304-3770(01)00151-6.
[39] Verhagen JHG, Nienhuis PH. A simulation-model of production, seasonal-changes in biomass and distribution of eelgrass (*Zostera marina*) in lake Grevelingen. Mar Ecol Ser 1983;10:187–95. http://dx.doi.org/10.3354/meps010187.
[40] Bach HK. A dynamic model describing the seasonal variations in growth and the distribution of eel grass (*Zostera marina*). Ecol Modell 1993;65:31–50. http://dx.doi.org/10.1016/0304-3800(93)90125-c.
[41] Biber PD, Gallegos CL, Kenworthy WJ. Calibration of a bio-optical model in the North River, North Carolina (Albemarle–Pamlico Sound): a tool to evaluate water quality impacts on seagrasses. Estuaries Coasts 2008;31:177–91. http://dx.doi.org/10.1007/s12237-007-9023-6.

[42] Gallegos CL. Calculating optical water quality targets to restore and protect submersed aquatic vegetation: overcoming problems in partitioning the diffuse attenuation coefficient for photosynthetically active radiation. Estuaries 2001;24:381–97. http://dx.doi.org/10.2307/1353240.
[43] Oertel G. Hypsographic, hydro-hypsographic and hydrological analysis of coastal bay environments, Great Machipongo Bay. J Coast Res 2001;17:775–83.
[44] Orth RJ, Carruthers TJB, Dennison WC, Duarte CM, Fourqurean JW, Heck KL, et al. A global crisis for seagrass ecosystems. Bioscience 2006;56:987–96. http://dx.doi.org/10.1641/0006-3568(2006)56[987:agcfse]2.0.co;2.
[45] Orth R, McGlathery K. Eelgrass recovery in the coastal bays of the Virginia Coast Reserve, USA. Mar Ecol Prog Ser 2012;448:173–6. http://dx.doi.org/10.3354/meps09596.
[46] McGlathery K, Reynolds L, Cole L, Orth R, Marion SR, Schwarzschild A. Recovery trajectories during state change from bare sediment to eelgrass dominance. Mar Ecol Prog Ser 2012;448:209–21. http://dx.doi.org/10.3354/meps09574.
[47] Fagherazzi S, Wiberg PL. Importance of wind conditions, fetch, and water levels on wave-generated shear stresses in shallow intertidal basins. J Geophys Res Earth Surf 2009;114. http://dx.doi.org/10.1029/2008JF001139.
[48] Lawson S.E. Sediment suspension as a control on light availability in a coastal lagoon. 2004.
[49] Hornberger G.M. Elements of physical hydrology. JHU Press; 1998.
[50] Luhar M, Nepf HM. From the blade scale to the reach scale: a characterization of aquatic vegetative drag. Adv Water Resour 2013;51:305–16. http://dx.doi.org/10.1016/j.advwatres.2012.02.002.
[51] Rominger JJT, Nepf HH. Flow adjustment and interior flow associated with a rectangular porous obstruction. J Fluid Mech 2011;680:636–59. http://dx.doi.org/10.1017/jfm.2011.199.
[52] Lefebvre A, Thompson CEL, Amos CL. Influence of *Zostera marina* canopies on unidirectional flow, hydraulic roughness and sediment movement. Cont Shelf Res 2010;30:1783–94. http://dx.doi.org/10.1016/j.csr.2010.08.006.
[53] Markfort CD. Wind sheltering of a lake by a tree canopy or bluff topography. Water Resour Res 2010;46:W03530. http://dx.doi.org/10.1029/2009wr007759.
[54] Walker IJ. Simulation and measurement of surface shear stress over isolated and closely spaced transverse dunes in a wind tunnel. Earth Surf Process Landforms 2003;28:1111–24. http://dx.doi.org/10.1002/esp.520.
[55] Folkard A. Flow regimes in gaps within stands of flexible vegetation: laboratory flume simulations. Environ Fluid Mech 2011;11:289–306. http://dx.doi.org/10.1007/s10652-010-9197-5.
[56] Okin GS. A new model of wind erosion in the presence of vegetation. J Geophys Res 2008;113. http://dx.doi.org/10.1029/2007JF000758.
[57] Young IRR, Verhagen LAA. The growth of fetch limited waves in water of finite depth. 1. Total energy and peak frequency. Coast Eng 1996;29:47–78. http://dx.doi.org/10.1016/S0378-3839(96)00006-3.
[58] Fonseca MS, Cahalan JA. A preliminary evaluation of wave attenuation by four species of seagrass. Estuar Coast Shelf Sci 1992;35:565–76. http://dx.doi.org/10.1016/S0272-7714(05)80039-3.
[59] Méndez FJ, Losada IJ, Losada MA. Hydrodynamics induced by wind waves in a vegetation field. J Geophys Res Ocean 1999;104:18383–96. http://dx.doi.org/10.1029/1999JC900119.
[60] Patil S, Singh VP. Hydrodynamics of wave and current vegetation interaction. J Hydrol Eng 2009;14:1320–33. http://dx.doi.org/10.1061/(ASCE)HE.1943-5584.0000125.
[61] Lowe RJ. Oscillatory flow through submerged canopies: 1. Velocity structure. J Geophys Res 2005;110:C10016. http://dx.doi.org/10.1029/2004JC002788.
[62] Lowe R, Falter J. Spectral wave flow attenuation within submerged canopies: Implications for wave energy dissipation. Ocean (1978–2012) 2007;112(C5). http://dx.doi.org/10.1029/2006jc003605.
[63] Van der Heide T, van Nes EH, Geerling GW, Smolders AJP, Bouma TJ, Katwijk MM. Positive feedbacks in seagrass ecosystems: implications for success in conservation and restoration. Ecosystems 2007;10:1311–22. http://dx.doi.org/10.1007/s10021-007-9099-7.
[64] Hansen J, Reidenbach M. Wave and tidally driven flows in eelgrass beds and their effect on sediment suspension. Mar Ecol Prog Ser 2012;448:271–87. http://dx.doi.org/10.3354/meps09225.
[65] Harris CK, Wiberg PL. Approaches to quantifying long-term continental shelf sediment transport with an example from the Northern California STRESS mid-shelf site. Cont Shelf Res 1997;17:1389–418. http://dx.doi.org/10.1016/s0278-4343(97)00017-4.
[66] Chaudhry MH. Open-channel flow. Boston, MA: Springer US; 2008. http://dx.doi.org/10.1007/978-0-387-68648-6.
[67] Smith JD, McLean SR. Spatially averaged flow over a wavy surface. J Geophys Res 1977;82:1735–46. http://dx.doi.org/10.1029/JC082i012p01735.
[68] Dorrell RM, Hogg AJ. Length and time scales of response of sediment suspensions to changing flow conditions. J Hydraulic Eng 2012;138:430–9. http://dx.doi.org/10.1061/(ASCE)HY.1943-7900.0000532.
[69] Toffolon M, Vignoli G. Suspended sediment concentration profiles in nonuniform flows: Is the classical perturbative approach suitable for depth-averaged closures? Water Resour Res 2007;43. http://dx.doi.org/10.1029/2006WR005183.
[70] Rouse H. Modern conceptions of the mechanics or fluid turbulence. Trans Am Soc Civ Eng 1937;102:463–505.
[71] Duarte CM. The future of seagrass meadows. Environ Conserv 2002;29:192–206. http://dx.doi.org/10.1017/S0376892902000127.
[72] Moore K.A., Jarvis J.C. Environmental factors affecting recent summertime eelgrass diebacks in the Lower Chesapeake Bay: implications for long-term persistence. J Coast Res 2008:135–147. doi:10.2112/si55-014.
[73] Zambrano L, Scheffer M, Martínez-Ramos M. Catastrophic response of lakes to benthivorous fish introduction. Oikos 2001;94(2):344–50. http://dx.doi.org/10.1034/j.1600-0706.2001.940215.x.
[74] Scheffer M. Fish facilitate wave resuspension of sediment. Limnology 2003;48(5):1920–6. http://dx.doi.org/10.4319/lo.2003.48.5.1920.
[75] Van De Koppel J, Herman PMJ, Thoolen P, Heip CHR. Do alternate stable states occur in natural ecosystems? Evidence from a tidal flat. Ecology 2001;82:3449–61. http://dx.doi.org/10.2307/2680164.
[76] Bell SS. Dynamics of a subtropical seagrass landscape: links between disturbance and mobile seed banks. Landsc Ecol 2008;23:67–74. http://dx.doi.org/10.1007/s10980-007-9137-z.
[77] Boese BL, Kaldy JE, Clinton PJ, Eldridge PM, Folger CL. Recolonization of intertidal *Zostera marina* L. (eelgrass) following experimental shoot removal. J Exp Mar Bio Ecol 2009;374:69–77. http://dx.doi.org/10.1016/j.jembe.2009.04.011.
[78] Vandenbruwaene W, Temmerman S, Bouma TJ, Klaassen PC, de Vries MB, Callaghan DP, et al. Flow interaction with dynamic vegetation patches: implications for biogeomorphic evolution of a tidal landscape. J Geophys Res Earth Surf 2011;116. http://dx.doi.org/10.1029/2010JF001788.
[79] Hu Z, Suzuki T, Zitman T, Uittewaal W, Stive M. Laboratory study on wave dissipation by vegetation in combined current–wave flow. Coastal Eng 2014;88:131–42. http://dx.doi.org/10.1016/j.coastaleng.2014.02.009.
[80] Infantes E, Orfila A, Simarro G. Effect of a seagrass (*Posidonia oceanica*) meadow on wave propagation. Mar Ecol 2012;456:63–72. http://dx.doi.org/10.3354/meps09754.
[81] Luhar M. Wave-induced velocities inside a model seagrass bed. J Geophys Res 2010;115. http://dx.doi.org/10.1029/2010jc006345.
[82] Bradley K. Relative velocity of seagrass blades: implications for wave attenuation in low-energy environments. J Geophys Res 2009;114:F01004. http://dx.doi.org/10.1029/2007jf000951.
[83] Lowe RJ. Oscillatory flow through submerged canopies: 1. Velocity structure. J Geophys Res 2005;110:C10016. http://dx.doi.org/10.1029/2004jc002788.
[84] Zimmerman R, Kohrs D. Impacts of CO_2 enrichment on productivity and light requirements of eelgrass. Plant Physiology 1997;115(2):599–607. http://dx.doi.org/10.1104/pp.115.2.599.
[85] Zimmerman R, Smith R, Alberte R. Thermal acclimation and whole-plant carbon balance in *Zostera marina* L. (eelgrass). J Exp Mar 1989;130(2):93–109. http://dx.doi.org/10.1016/0022-0981(89)90197-4.
[86] Burke M, Dennison W, Moore K. Non-structural carbohydrate reserves of eelgrass *Zostera marina*. Mar Ecol Prog Ser 1996;137:195–201. http://dx.doi.org/10.3354/meps137195.
[87] Walker B, Salt D. Resilience thinking: sustaining ecosystems and people in a changing world 2006.